



Article

A Numerical Solution of Generalized Caputo Fractional Initial Value Problems

Rania Saadeh ^{1,*} , Mohamed A. Abdoon ^{2,3} , Ahmad Qazza ¹ and Mohammed Berir ^{3,4}¹ Department of Mathematics, Zarqa University, Zarqa 13110, Jordan² Department of Basic Sciences (Mathematics) Deanship of Common First Year, Shaqra University, Riyadh 15342, Saudi Arabia³ Department of Mathematics, Faculty of Science, Bakht Al-Ruda University, Duwaym 28812, White Nile State, Sudan⁴ Department of Mathematics, Faculty of Science and Arts, Al-Baha University, Baljurashi 1988, Saudi Arabia

* Correspondence: rsaadeh@zu.edu.jo

Abstract: In this article, the numerical adaptive predictor corrector (Apc-ABM) method is presented to solve generalized Caputo fractional initial value problems. The Apc-ABM method was utilized to establish approximate series solutions. The presented technique is considered to be an extension to the original Adams–Bashforth–Moulton approach. Numerical simulations and figures are presented and discussed, in order to show the efficiency of the proposed method. In the future, we anticipate that the provided generalized Caputo fractional derivative and the suggested method will be utilized to create and simulate a wide variety of generalized Caputo-type fractional models. We have included examples to demonstrate the accuracy of the present method.

Keywords: numerical solution; the Apc-ABM method; Caputo derivative; chaos

MSC: 26A33; 65P20



Citation: Saadeh, R.; A. Abdoon, M.; Qazza, A.; Berir, M. A Numerical Solution of Generalized Caputo Fractional Initial Value Problems. *Fractal Fract.* **2023**, *7*, 332. <https://doi.org/10.3390/fractalfract7040332>

Academic Editors: Ahmet Bekir, Adem Cevikel and Emad Zahran

Received: 15 March 2023

Revised: 29 March 2023

Accepted: 7 April 2023

Published: 17 April 2023



Copyright: © 2023 by the authors. Licensee MDPI, Basel, Switzerland. This article is an open access article distributed under the terms and conditions of the Creative Commons Attribution (CC BY) license (<https://creativecommons.org/licenses/by/4.0/>).

1. Introduction

The application of fractional calculus to represent a range of different physical scientific fields, such as diffusion, control, and viscoelasticity, has contributed to the field of applied mathematics, which has risen in popularity over the last several decades. In many branches of engineering and the study of physics, see [1–5], fractional differential equations are commonplace. Many methods have been tried and tested in an effort to investigate and resolve fractional differential equations [6–12]. Together with advances in symbolic programming and new computing algorithms, the past few decades have seen the discovery of a plethora of novel methods for solving nonlinear partial differential equations. In addition, classic software such as Mathematica, MATLAB, and Maple have received several updates and remain potent resources. However, there has been progress in the mathematical foundations of solution techniques, and new methods have been developed to solve a wide range of problems that are built on top of nonlinear partial differential equations [13–16]. The primary techniques in the literature include providing a pseudo-operational collocation scheme to deal with the solution of the variable-order time–space fractional KdV–Burgers–Kuramoto equation [17]. Several methodologies have been used to tackle challenges in management, economics, and biology, including physics and engineering [18–24]. The use of fractional integrals allows for the definition of a class of fractional derivatives. Some examples of this class are Riemann–Liouville, Hadamard, and Caputo.

The Riemann–Liouville fractional integral of order $\alpha > 0$ is given by the following:

$$I_{a+}^{\alpha} f(t) = \frac{1}{\Gamma(\alpha)} \int_a^t (t-s)^{\alpha-1} f(s) ds, \quad t > a. \quad (1)$$

Using the definition of the fractional integral in (1), the Caputo fractional derivative, Caputo fractional derivative, and the Riemann–Liouville fractional derivative with $\alpha > 0$ are given by the following:

$$\begin{aligned} {}^R D_{a+}^{\alpha} f(t) &= D^m I_{a+}^{m-\alpha} f(t) = \frac{1}{\Gamma(m-\alpha)} \frac{d^m}{dt^m} \int_a^t (t-s)^{m-\alpha-1} f(s) ds, \quad t > a, \\ {}^C D_{a+}^{\alpha} f(t) &= I_{a+}^{m-\alpha} D^m f(t) = \frac{1}{\Gamma(m-\alpha)} \int_a^t (t-s)^{m-\alpha-1} f^{(m)}(s) ds, \quad t > a, \end{aligned} \quad (2)$$

where $m-1 < \alpha \leq m$ and $m \in \mathbb{N}$. See [25].

The strength of this study is this method, which can be applied to a wide range of equations and dynamical systems. The main result of this research are some examples we created and simulated, the Bernoulli equation and fractional new chaos system of generalized Caputo-type fractional models. We included examples to show how accurate the presented method is. The following is the structure of this article: Section 2 consists of definitions of generalized fractional derivatives; in Section 3, we explain the steps of the algorithm of the Apc-ABM method; in Section 4, we implement the Apc-ABM method for solving initial value problems numerically, using the suggested extended Caputo fractional derivative; finally, the conclusions of this article are presented.

2. Basic Definitions

In this section, we briefly review the fractional operators, generalized operator derivatives used throughout our analysis.

Definition 1. If f is a continuous function, then the generalized fractional integral denoted by $I_{a+}^{\alpha, \rho} f(t)$, $\alpha > 0$, and $\rho > 0$, is given by the following:

$$I_{a+}^{\alpha, \rho} f(t) = \frac{\rho^{1-\alpha}}{\Gamma(\alpha)} \int_a^t s^{\rho-1} (t^{\rho} - s^{\rho})^{\alpha-1} f(s) ds, \quad \alpha > 0, \quad t > a. \quad (3)$$

For $m-1 < \alpha \leq m$ where $m \in \mathbb{N}$, see [26].

Definition 2. If f is a continuous function, then the generalized Riemann–Liouville fractional derivative denoted by $D_{a+}^{\alpha, \rho} f(t)$, of order $\alpha > 0$ is given by the following:

$${}^R D_{a+}^{\alpha, \rho} f(t) = \frac{\rho^{\alpha-m+1}}{\Gamma(m-\alpha)} \left(t^{1-\rho} \frac{d}{dt} \right)^m \int_a^t s^{\rho-1} (t^{\rho} - s^{\rho})^{m-\alpha-1} f(s) ds, \quad t > a \geq 0. \quad (4)$$

Definition 3. If f is a continuous function, then the generalized Caputo fractional derivative denoted by ${}^C D_{a+}^{\alpha, \rho} f(t)$, of order $\alpha > 0$ is given by the following:

$${}^C D_{a+}^{\alpha, \rho} f(t) = \left({}^R D_{a+}^{\alpha, \rho} \left[f(x) - \sum_{n=0}^{m-1} \frac{f^{(n)}(a)}{n!} (x-a)^n \right] \right)(t), \quad t > a \geq 0, \quad (5)$$

where $m = \lceil \alpha \rceil$ and $\rho > 0$. In case of $0 < \alpha \leq 1$, see [27].

$${}^C D_{a+}^{\alpha, \rho} f(t) = \frac{\rho^{\alpha}}{\Gamma(1-\alpha)} \int_a^t (t^{\rho} - s^{\rho})^{-\alpha} f'(s) ds, \quad 0 < \alpha \leq 1, \quad t > a \geq 0. \quad (6)$$

Definition 4. The new generalized Caputo fractional derivative operator, $\mathcal{D}_{a+}^{\alpha,\rho}$, $\alpha > 0$ is given by the following:

$$(\mathcal{D}_{a+}^{\alpha,\rho} f)(t) = \frac{\rho^{\alpha-m+1}}{\Gamma(m-\alpha)} \int_a^t s^{\rho-1} (t^\rho - s^\rho)^{m-\alpha-1} \left(s^{1-\rho} \frac{d}{ds} \right)^m f(s) ds, \quad t > a, \quad (7)$$

where $\rho > 0$, $a \geq 0$, and $m-1 < \alpha < m$.

3. Algorithm of the Apc-ABM Method

In this section, we present an algorithm of the Apc-ABM technique, which we refer to as the adaptive Apc-ABM method, in order to efficiently provide numerical solutions for initial value problems with the generalized Caputo fractional derivative, as follows:

$$\begin{cases} \mathcal{D}_{a+}^{\alpha,\rho} y(t) = f(t, y(t)), & t \in [0, T], \\ y^{(k)}(a) = y_0^k, & k = 0, 1, \dots, \lceil \alpha \rceil, \end{cases} \quad (8)$$

where $\mathcal{D}_{a+}^{\alpha,\rho}$ is the proposed generalized Caputo fractional derivative operator given in Equation (7). Then, for $m-1 < \alpha \leq m$, $a \geq 0$, $\rho > 0$ and $y \in C^m([a, T])$, the initial value problem (7) is equivalent; we obtain the following:

$$y(t) = u(t) + \frac{\rho^{1-\alpha}}{\Gamma(\alpha)} \int_a^t s^{\rho-1} (t^\rho - s^\rho)^{\alpha-1} f(s, y(s)) ds, \quad (9)$$

where

$$u(t) = \sum_{n=0}^{m-1} \frac{1}{\rho^n n!} (t^\rho - a^\rho)^n \left[\left(x^{1-\rho} \frac{d}{dx} \right)^n y(x) \right] \Big|_{x=a} \quad (10)$$

On the assumption that the function f has a unique solution in some interval $[a, T]$, we divide the interval into N unequal subintervals $\{[t_k, t_{k+1}], k = 0, 1, \dots, N-1\}$ using mesh points, as follows:

$$\begin{cases} t_0 = a, \\ t_{k+1} = (t_k^\rho + h)^{1/\rho}, & k = 0, 1, \dots, N-1, \end{cases} \quad (11)$$

where $h = \frac{T^\rho - a^\rho}{N}$. Now, to numerically solve the initial value problem, we will build approximations $y_k, k = 0, 1, \dots, N$. If we have previously assessed the approximations $y(t_j)$ and $y_j \approx y(t_j) (j = 1, 2, \dots, k)$, we wish to use the integral equation to generate the approximation $y_{k+1} \approx y(t_{k+1})$.

$$y(t_{k+1}) = u(t_{k+1}) + \frac{\rho^{1-\alpha}}{\Gamma(\alpha)} \int_a^{t_{k+1}} s^{\rho-1} (t_{k+1}^\rho - s^\rho)^{\alpha-1} f(s, y(s)) ds. \quad (12)$$

Making the following substitution:

$$z = S^\rho, \quad (13)$$

We obtain the following:

$$y(t_{k+1}) = u(t_{k+1}) + \frac{\rho^{-\alpha}}{\Gamma(\alpha)} \int_{a^\rho}^{t_{k+1}^\rho} (t_{k+1}^\rho - z)^{\alpha-1} f(z^{1/\rho}, y(z^{1/\rho})) dz. \quad (14)$$

That is, we obtain the following:

$$y(t_{k+1}) = u(t_{k+1}) + \frac{\rho^{-\alpha}}{\Gamma(\alpha)} \sum_{j=0}^k \int_{t_j^\rho}^{t_{j+1}^\rho} (t_{k+1}^\rho - z)^{\alpha-1} f(z^{1/\rho}, y(z^{1/\rho})) dz. \quad (15)$$

Next, using the trapezoidal quadrature procedure with respect to the weight function $(t_{k+1}^\rho - \cdot)^{\alpha-1}$ to approximate the integrals in the right-hand side of Equation (15), we derive the following corrector formula for $y(t_{k+1}), k = 0, 1, \dots, N-1$:

$$y(t_{k+1}) \approx u(t_{k+1}) + \frac{\rho^{-\alpha} h^\alpha}{\Gamma(\alpha+2)} \sum_{j=0}^k a_{j,k+1} f(t_j, y(t_j)) + \frac{\rho^{-\alpha} h^\alpha}{\Gamma(\alpha+2)} f(t_{k+1}, y(t_{k+1})), \quad (16)$$

where

$$a_{j,k+1} = \begin{cases} k^{\alpha+1} - (k-\alpha)(k+1)^\alpha & \text{if } j=0, \\ (k-j+2)^{\alpha+1} + (k-j)^{\alpha+1} - 2(k-j+1)^{\alpha+1} & \text{if } 1 \leq j < k. \end{cases} \quad (17)$$

The final stage of our technique is to replace the amount $y(t_{k+1})$ on the right side of Formula (14) with the predictor value $y^P(t_{k+1})$ produced by using the one-step Adams–Bashforth method to the integral Equation (14). In this situation, substituting the function $f(z^{1/\rho}, y(z^{1/\rho}))$ at each integral in Equation (16) with the amount $f(t_j, y(t_j))$ yields the following:

$$\begin{aligned} y^P(t_{k+1}) &\approx u(t_{k+1}) + \frac{\rho^{-\alpha}}{\Gamma(\alpha)} \sum_{j=0}^k \int_{t_j^\rho}^{t_{j+1}^\rho} (t_{k+1}^\rho - z)^{\alpha-1} f(t_j, y(t_j)) dz \\ &= u(t_{k+1}) + \frac{\rho^{-\alpha} h^\alpha}{\Gamma(\alpha+1)} \sum_{j=0}^k [(k+1-j)^\alpha - (k-j)^\alpha] f(t_j, y(t_j)). \end{aligned} \quad (18)$$

Therefore, the formula fully describes the Apc-ABM for assessing the approximation $y_{k+1} \approx y(t_{k+1})$, as follows:

$$y_{k+1} \approx u(t_{k+1}) + \frac{\rho^{-\alpha} h^\alpha}{\Gamma(\alpha+2)} \sum_{j=0}^k a_{j,k+1} f(t_j, y_j) + \frac{\rho^{-\alpha} h^\alpha}{\Gamma(\alpha+2)} f(t_{k+1}, y_{k+1}^P), \quad (19)$$

where $y_j \approx y(t_j), j = 0, 1, \dots, k$, and the predicted value $y_{k+1}^P \approx y^P(t_{k+1})$ can be determined as described in Equation (18) with the weights $a_{j,k+1}$ being defined according to (35). The proposed adaptive Apc-ABM method uses non-uniform grid points:

$\{t_{j+1} = (t_j^\rho + h)^\rho : j = 0, 1, \dots, N-1\}$ with $t_0 = a$ and $h = \frac{T^\rho - a^\rho}{N}$, where N is a natural number. For this research, we should mention that we cannot apply the Apc-ABM approach to solve initial value problems that are defined with the generalized Caputo fractional derivative, if we use a uniform grid as stated in [28].

4. Applications

In this section, we explore the usefulness of the Apc-ABM method for solving initial value problems numerically with the suggested extended Caputo fractional derivative. As such, we resorted to numerical simulations to examine solutions to apply our test issues.

Problem 1. Let us consider the fractional Bernoulli equation of the following form:

$$\mathcal{D}_0^{\alpha,\rho} y(t) = 2y(t) - 4y^2(t), \quad t > 0, \quad 0 < \alpha \leq 1, \quad (20)$$

This is associated with the condition $y(0) = 1$, where $\mathcal{D}_0^{\alpha,\rho}$ is the generalized Caputo fractional derivative, presented in Equation (7) of parameters α and ρ . The solution of the Bernoulli Equation (20), with $\alpha = 1$ and $\rho = 1$, is as follows:

$$y(t) = \frac{-1}{e^{-2t} - 1}, \quad (21)$$

under $y(0) = 0$, where $\mathcal{D}_0^{\alpha,\rho}$ is defined by Equation (7) with parameters α and ρ . When $\alpha = 1$ and $\rho = 1$, the Bernoulli Equation (20) has an exact solution according to the proposed Apc-ABM method, for some $T > 0$. We show these results in the following tables.

In Table 1, we provide numerical results from our Apc-ABM method to the fractional Bernoulli Equation (20) when $\alpha = 1$ and $\rho = 1$ at $t = 6, t = 8$, and $t = 10$. Table 2 displays numerical results; our technique yielded numerical answers that precisely matched the solutions well (y_{Exact}). The accuracy improved as the step size h was reduced. We provided numerical results from our the Apc-ABM method to the fractional Bernoulli Equation (20) at $t = 6, t = 8$, and $t = 10$, correspondingly for a variety of values of α and ρ . The numerical stability of the Apc-ABM method may be seen in the convergence of the findings shown in Tables 3 and 4.

Table 1. Numerical simulations to solve Equation (20) when $\alpha = 1$ and $\rho = 1$.

| h | $t = 6$ | $t = 8$ | $t = 10$ |
|-------------|--------------|--------------|--------------|
| 1/20 | 0.5000007458 | 0.5000000179 | 0.5000000001 |
| 1/40 | 0.5000010853 | 0.5000000179 | 0.5000000002 |
| 1/80 | 0.5000012953 | 0.5000000225 | 0.5000000003 |
| 1/160 | 0.5000014116 | 0.5000000252 | 0.5000000004 |
| 1/320 | 0.5000014728 | 0.5000000266 | 0.5000000004 |
| 1/640 | 0.5000015041 | 0.5000000273 | 0.5000000004 |
| 1/1280 | 0.5000015200 | 0.5000000277 | 0.5000000005 |
| y_{Exact} | 0.5000015360 | 0.5000000281 | 0.5000000005 |

Table 2. Numerical simulations to solve Equation (20) when $t = 6$.

| h | $\alpha = 1, \rho = 0.9$ | $\alpha = 1, \rho = 0.8$ | $\alpha = 1, \rho = 0.7$ |
|--------|--------------------------|--------------------------|--------------------------|
| 1/20 | 0.500000002050 | 0.500000024787 | 0.500000026437 |
| 1/40 | 0.500000004467 | 0.500000044735 | 0.5000000328657 |
| 1/80 | 0.500000006389 | 0.500000058854 | 0.5000000365178 |
| 1/160 | 0.500000007587 | 0.500000067188 | 0.5000000384626 |
| 1/320 | 0.500000008255 | 0.500000071708 | 0.5000000394658 |
| 1/640 | 0.500000008607 | 0.500000074060 | 0.5000000399752 |
| 1/1280 | 0.500000008788 | 0.500000075259 | 0.5000000264437 |

Table 3. Numerical simulations to solve Equation (20) when $t = 8$.

| h | $\alpha = 1, \rho = 0.9$ | $\alpha = 1, \rho = 0.8$ | $\alpha = 1, \rho = 0.7$ |
|--------|--------------------------|--------------------------|--------------------------|
| 1/20 | 0.500000000004 | 0.500000000118 | 0.5000000002731 |
| 1/40 | 0.500000000011 | 0.500000000256 | 0.5000000003624 |
| 1/80 | 0.500000000018 | 0.500000000366 | 0.5000000004156 |
| 1/160 | 0.500000000023 | 0.500000000435 | 0.5000000004447 |
| 1/320 | 0.500000000026 | 0.500000000473 | 0.5000000004599 |
| 1/640 | 0.500000000028 | 0.500000000494 | 0.5000000004676 |
| 1/1280 | 0.500000000028 | 0.500000000504 | 0.5000000002731 |

In Figures 1 and 2, we sketch the solutions of Equation (20) with $T = 2.5$ that were obtained by the proposed method. We present approximate series solutions to Equation (20) with $T = 2.5$ from our the Apc-ABM method for various values of α and ρ . In Figure 2, for fixed α , in particular, for all three values of ρ , the solution $y(t)$ converged to the same limit. In Figure 3, we plot the numerical solutions of Equation (20) when $N = 300$ with a different value of α . Figure 4 presents comparison between the exact solution and the obtained numerical solution of Equation (20).

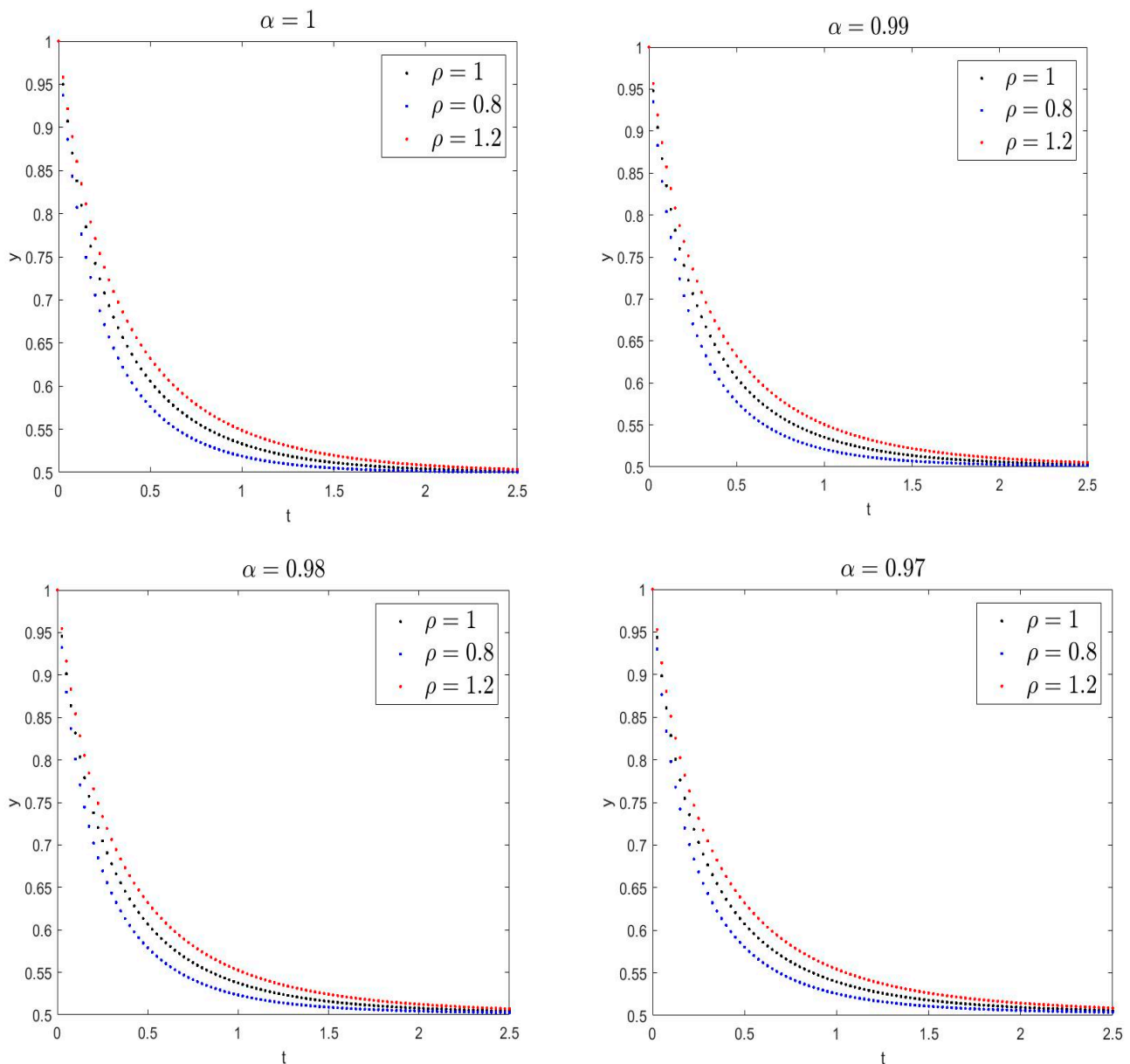


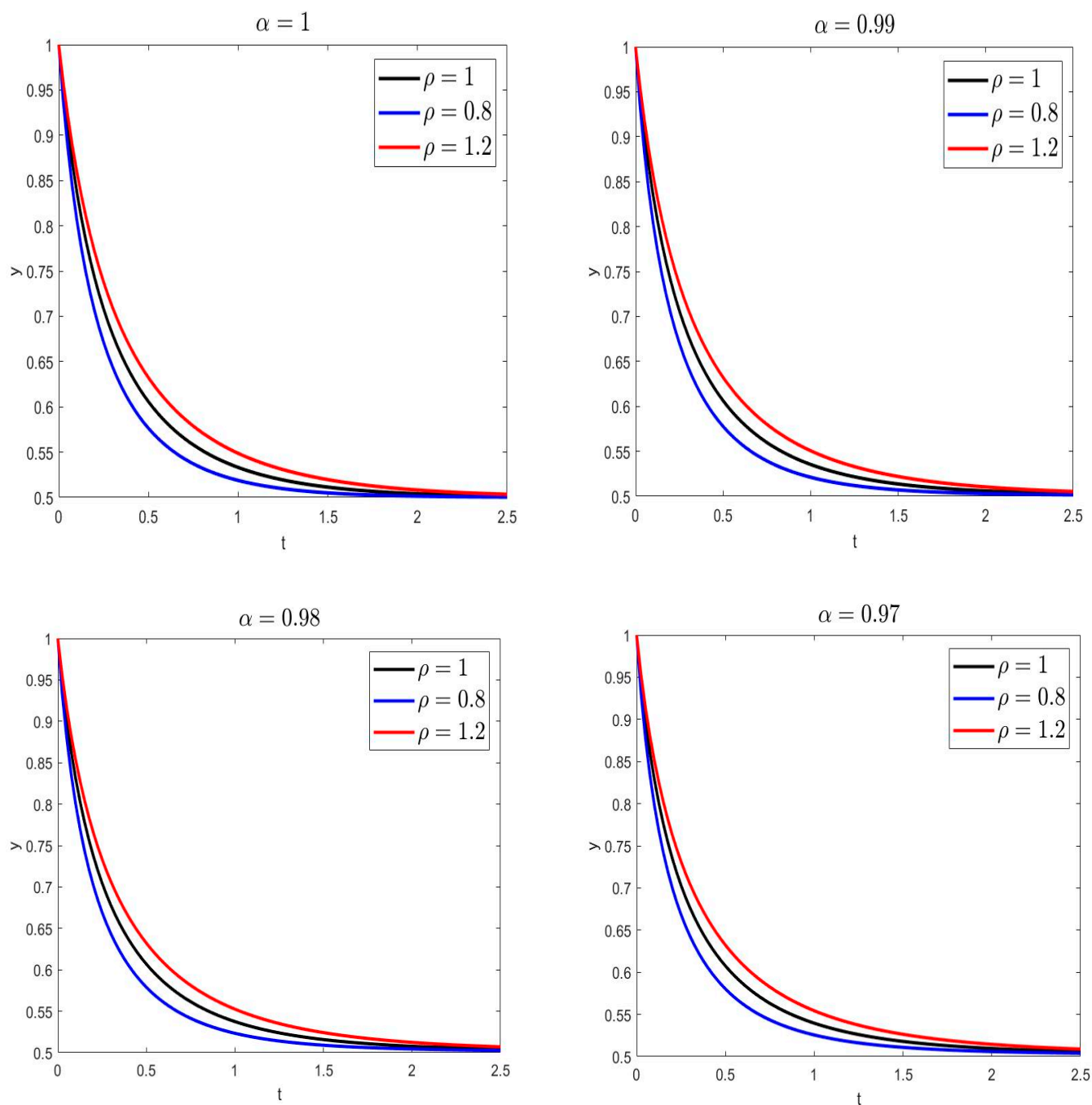
Figure 1. Plots of numerical solutions of Equation (20) when $N = 50$.

Table 4. The solutions of Problem 2 when $\alpha = 1$, $\rho = 1$ and $t = 0.1$.

| h . | x | y | z |
|--------|-----------|-----------|-----------|
| 1/160 | 0.5008215 | 0.8421048 | 0.5712066 |
| 1/320 | 0.5008442 | 0.8426022 | 0.5710918 |
| 1/640 | 0.5008554 | 0.8428494 | 0.5710347 |
| 1/1280 | 0.5008610 | 0.8429727 | 0.5710062 |

Table 4. Cont.

| $h.$ | x | y | z |
|---------|-----------|-----------|-----------|
| 1/2560 | 0.5008639 | 0.8430342 | 0.5709920 |
| 1/5120 | 0.5008653 | 0.8430649 | 0.5709849 |
| 1/10240 | 0.5008660 | 0.8430803 | 0.5709813 |
| 1/20480 | 0.5008663 | 0.8430880 | 0.5709795 |
| 1/40960 | 0.5008665 | 0.8430918 | 0.5709786 |
| 1/81920 | 0.5008666 | 0.8430957 | 0.5709778 |
| R K4 | 0.5008666 | 0.8430937 | 0.5709782 |

Figure 2. Plots of numerical solutions of Equation (20) when $N = 300$.

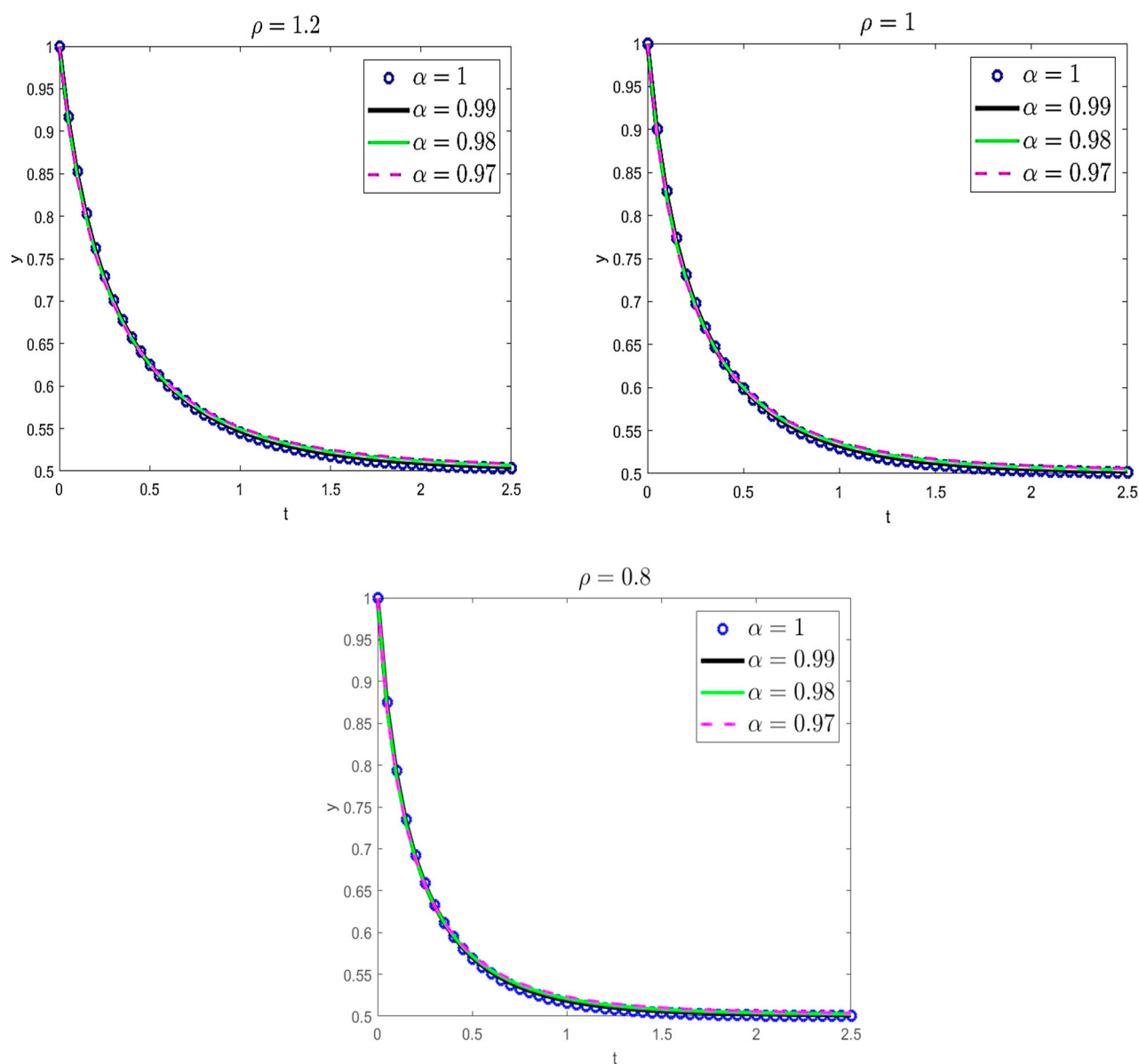


Figure 3. Plots of numerical solutions of Equation (20) when $N = 300$ with a different value of α .

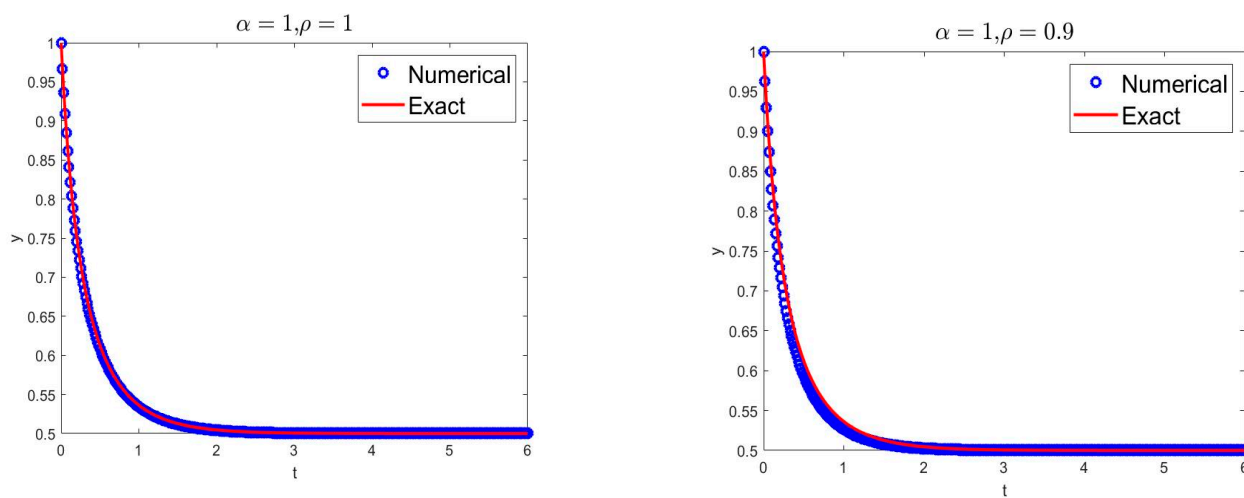


Figure 4. Cont.

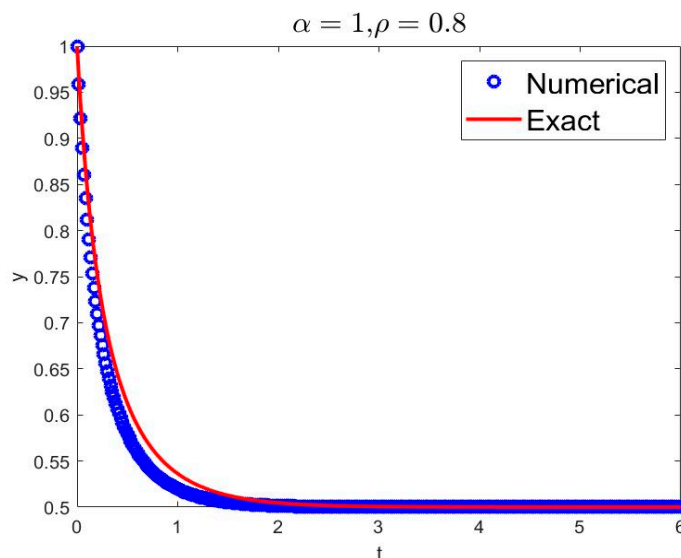


Figure 4. Comparison of exact and numerical solutions of Equation (20).

Problem 2. Let us consider the following fractional new chaos system:

$$\begin{cases} \mathcal{D}_0^{\alpha,\rho} x(t) = ax(t) - dyx(t), \\ \mathcal{D}_0^{\alpha,\rho} y(t) = -bx(t) - x(t)z(t), \\ \mathcal{D}_0^{\alpha,\rho} z(t) = x(t)y(t)z(t) - cz(t) + 4 \end{cases} \quad (22)$$

It is subject to the conditions $x(0) = 1$, $y(0) = 1$, and $z(0) = 1$, where $a, b, c \in \mathbb{R}$, $t > 0$, and $\mathcal{D}_0^{\alpha,\rho}$ is the generalized Caputo fractional derivative operator, with the values for the parameters of the previous model being $a = 1$, $b = 2$, $c = 1$, and $d = 1$.

We used Equation (19) for the approximations x_{k+1} , y_{k+1} , and z_{k+1} , and for $N \in \mathbb{N}$ and $T > 0$.

$$\begin{cases} x_{k+1} \approx x_0 + a \frac{\rho^{-\alpha} h^\alpha}{\Gamma(\alpha+2)} \sum_{j=0}^k a_{j,k+1} (y_j - x_j) + a \frac{\rho^{-\alpha} h^\alpha}{\Gamma(\alpha+2)} (y_{k+1}^P - x_{k+1}^P), \\ y_{k+1} \approx y_0 + \frac{\rho^{-\alpha} h^\alpha}{\Gamma(\alpha+2)} \sum_{j=0}^k a_{j,k+1} ((c-a)x_j - x_j z_j + cy_j) \\ \quad + \frac{\rho^{-\alpha} h^\alpha}{\Gamma(\alpha+2)} ((c-a)x_{k+1}^P - x_{k+1}^P z_{k+1}^P + cy_{k+1}^P), \\ z_{k+1} \approx z_0 + \frac{\rho^{-\alpha} h^\alpha}{\Gamma(\alpha+2)} \sum_{j=0}^k a_{j,k+1} (x_j y_j - bz_j) + \frac{\rho^{-\alpha} h^\alpha}{\Gamma(\alpha+2)} (x_{k+1}^P y_{k+1}^P - bz_{k+1}^P), \end{cases} \quad (23)$$

where $h = \frac{T^\rho}{N}$ and

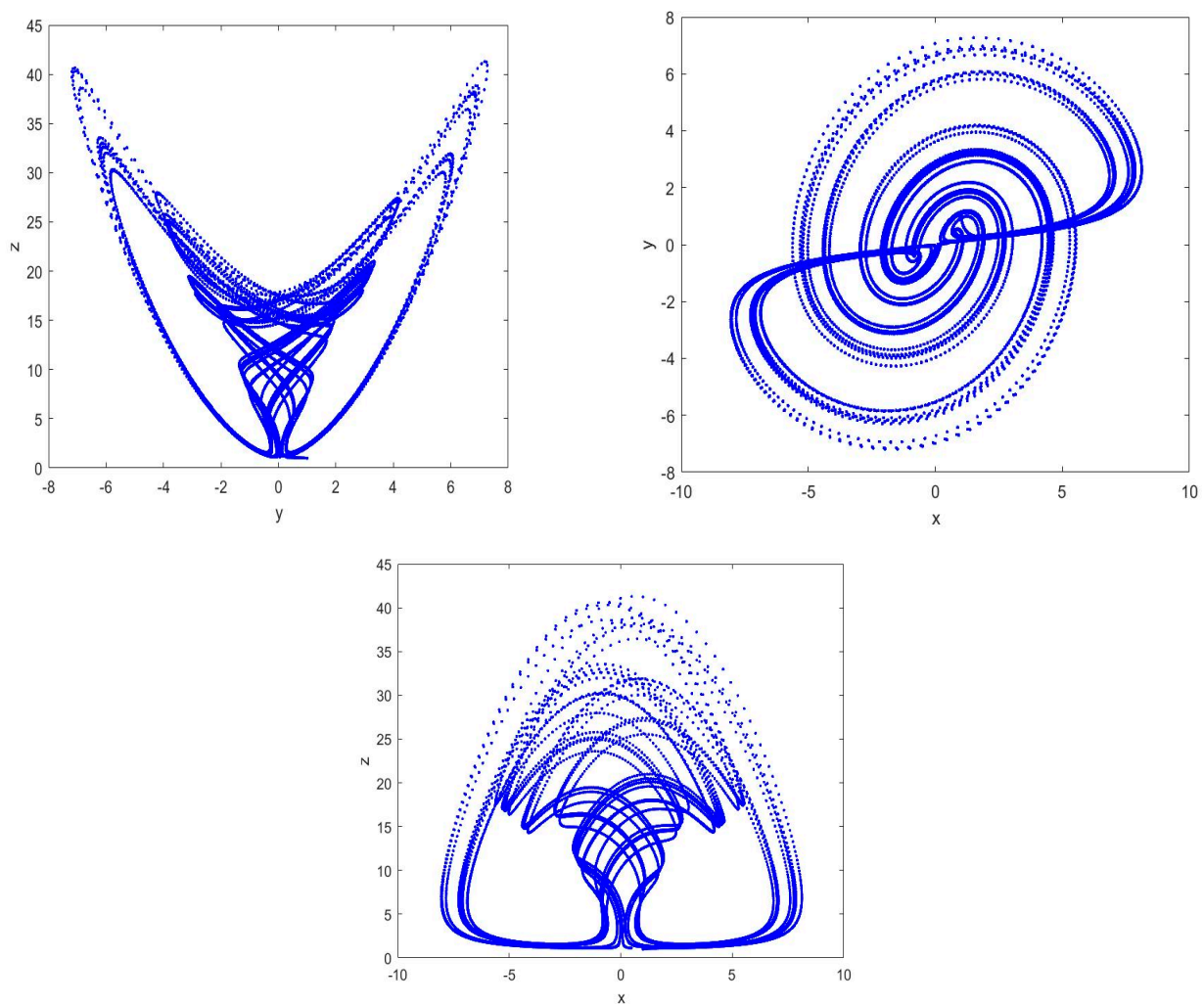
$$\begin{cases} x_{k+1}^P \approx x_0 + a \frac{\rho^{-\alpha} h^\alpha}{\Gamma(\alpha+1)} \sum_{j=0}^k [(k+1-j)^\alpha - (k-j)^\alpha] (y_j - x_j), \\ y_{k+1}^P \approx y_0 + \frac{\rho^{-\alpha} h^\alpha}{\Gamma(\alpha+1)} \sum_{j=0}^k [(k+1-j)^\alpha - (k-j)^\alpha] ((c-a)x_j - x_j z_j + cy_j), \\ z_{k+1}^P \approx z_0 + \frac{\rho^{-\alpha} h^\alpha}{\Gamma(\alpha+1)} \sum_{j=0}^k [(k+1-j)^\alpha - (k-j)^\alpha] (x_j y_j - bz_j). \end{cases} \quad (24)$$

In Table 4 below, we provide numerical results to the fractional Bernoulli Equation (21) when $\alpha = 1$, $\rho = 1$, $(a, b, c, d) = (1, 2, 1, 1)$, and $(x_0, y_0, z_0) = (1, 1, 1)$, using the Apc-ABM method and the RK4 method at $t = 2$ and $t = 4$. Table 5 presents numerical results. Note that the obtained numerical solutions in this problem are very close to those found by the RK4 technique when the step size h is made sufficiently small.

Table 5. The solutions of the Bernoulli Equation (22) when $\alpha = 1$, $\rho = 1$ and $t = 0.5$.

| h . | x | y | z |
|---------|-----------|-----------|-----------|
| 1/160 | 0.5350965 | 0.4761896 | 0.7847857 |
| 1/320 | 0.5351654 | 0.4772751 | 0.7844803 |
| 1/640 | 0.5351998 | 0.4778157 | 0.7843281 |
| 1/1280 | 0.5352170 | 0.4780855 | 0.7842521 |
| 1/2560 | 0.5352256 | 0.4782202 | 0.7842141 |
| 1/5120 | 0.5352299 | 0.4782876 | 0.7841952 |
| 1/10240 | 0.5352320 | 0.4783212 | 0.7841857 |
| 1/20480 | 0.5352331 | 0.4783381 | 0.7841809 |
| 1/40960 | 0.5352336 | 0.4783465 | 0.7841786 |
| 1/81920 | 0.5352339 | 0.4783507 | 0.7841774 |
| R K4 | 0.5352342 | 0.4783549 | 0.7841762 |

In Figures 5–7, we plot numerical solutions to Equation (20) when $(a, b, c, d) = (2.5, 9, 4, 1)$ and $(x_0, y_0, z_0) = (1, 1, 1)$. In these figures, we display the Equation (21) attractors obtained using the Apc-ABM method when $T = 40$ and $N = 1000$ for some values of the parameters α and ρ . It can be observed from Figures 5–7, that Equation (21), where $(a, b, c, d) = (2.5, 9, 4, 1)$, may show the same kind of chaotic attractor as its integer order when $(\alpha, \rho) = (0.95, 0.7)$, $(\alpha, \rho) = (0.95, 0.8)$, and $(\alpha, \rho) = (0.95, 0.9)$.

**Figure 5.** Chaotic attractor of Equation (22) when $(\alpha, \rho) = (0.95, 0.7)$.

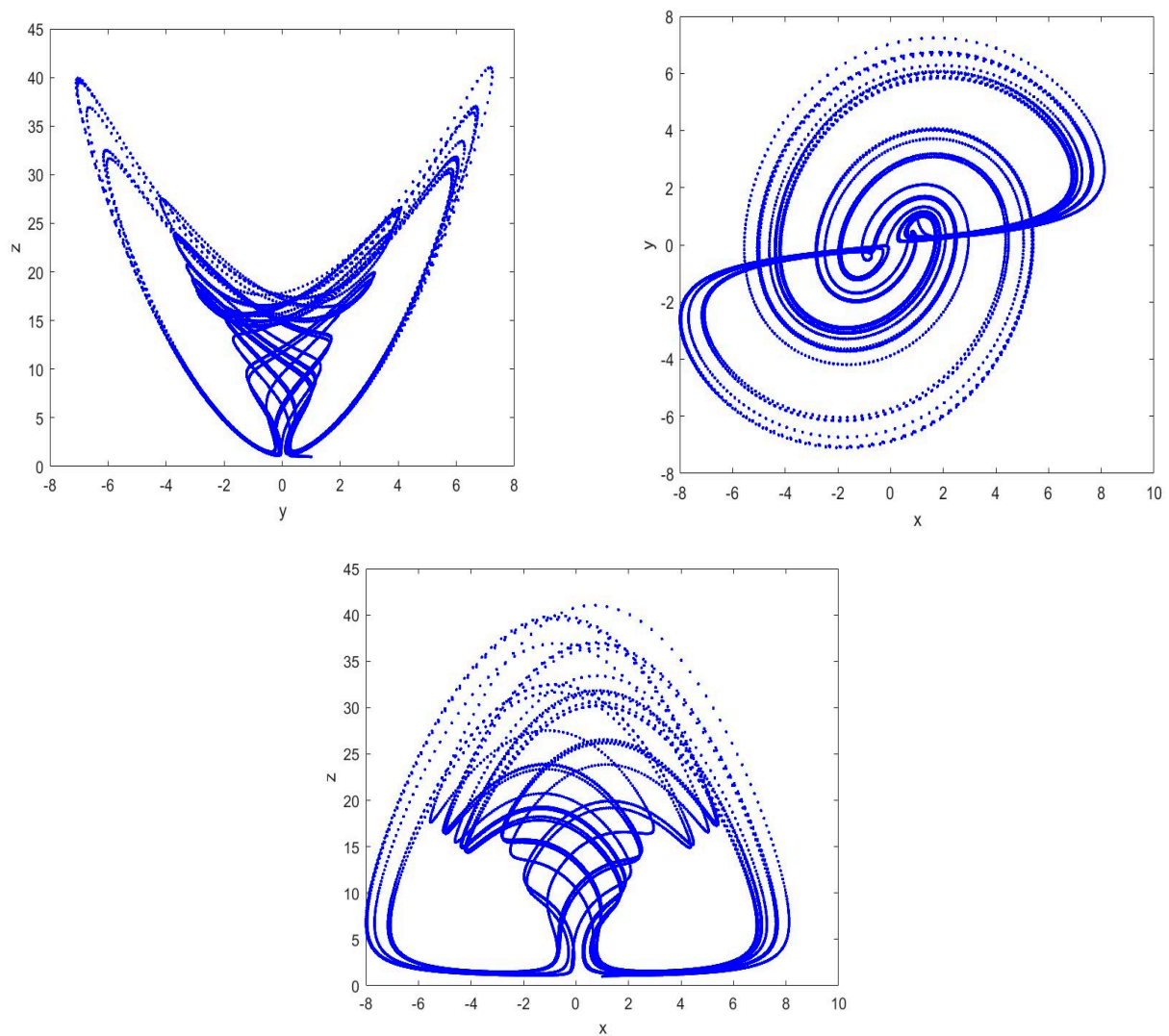


Figure 6. Chaotic attractor of Equation (22) when $(\alpha, \rho) = (0.95, 0.8)$.

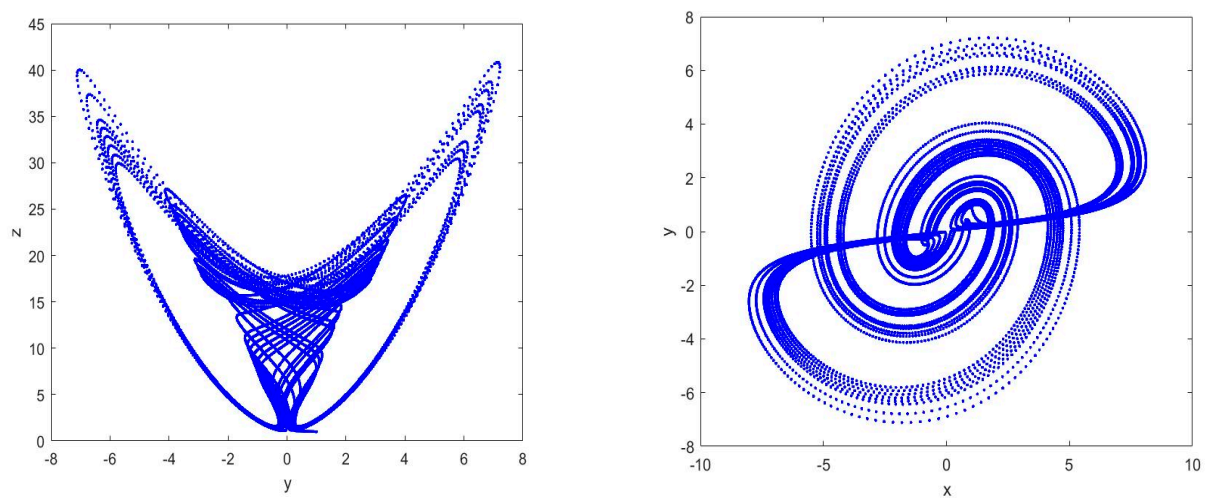


Figure 7. Cont.

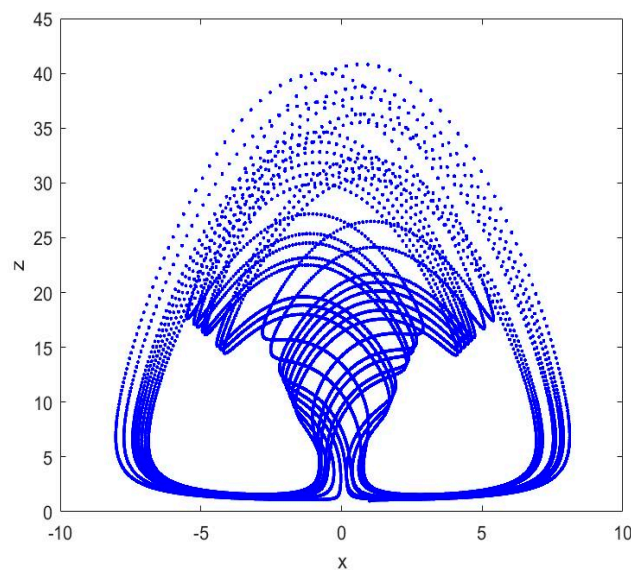


Figure 7. Chaotic attractor of Equation (22) when $(\alpha, \rho) = (0.95, 0.9)$.

Aperiodic long-term behavior, excessive sensitivity to starting conditions (SIC) on minute perturbations, and irregular responses due to nonlinearity are only a few examples of the complex nonlinear behaviors that emerge from a deterministic system to form the interesting phenomenon known as chaos; see [29,30]. Plasma oscillators [31], power transformers [32], coronary arteries of blood vessels [33], cancer, and tumor cells [34], among other real-world systems, can all experience chaos. For secure communications, chaos is tremendously helpful because of synchronization [35]. However, there are times when disorder needs to be controlled or suppressed, since it is unwelcome [36].

5. Discussion and Conclusions

This study successfully implemented the Apc-ABM method for numerically simulating systems of fractional differential equations, including the generalized Caputo fractional derivative. When the step size h decreased, the numerical simulations demonstrated that the provided technique yields numerical results that are extremely close to the accurate solutions in the integer case, or the approximate ones obtained by the RK4 method. In the case of fractions, the proposed analytical results demonstrate that the proposed procedure carries out its operations in a manner that is satisfactory in terms of its numerical stability. Using the suggested approach, we were able to effectively generate accurate approximation solutions and illustrate the dynamical behaviors of the systems under discussion. This research was carried out in the hope that it will be a useful resource for future applications and explorations of generalized Caputo fractional problems, and to investigate new methods such as those in [37–41].

Author Contributions: Conceptualization, R.S., M.A.A., A.Q. and M.B.; methodology, R.S., M.A.A., A.Q. and M.B.; software, R.S., M.A.A., A.Q. and M.B.; validation, R.S., M.A.A., A.Q. and M.B.; formal analysis, R.S., M.A.A., A.Q. and M.B.; investigation, R.S., M.A.A., A.Q. and M.B.; resources, R.S., M.A.A., A.Q. and M.B.; data curation, R.S., M.A.A., A.Q. and M.B.; writing—original draft preparation, R.S., M.A.A., A.Q. and M.B.; writing—review and editing, R.S., M.A.A., A.Q. and M.B.; visualization, R.S., M.A.A., A.Q. and M.B.; supervision, R.S., M.A.A., A.Q. and M.B.; project administration, R.S., M.A.A., A.Q. and M.B.; funding acquisition, R.S., M.A.A., A.Q. and M.B. All authors have read and agreed to the published version of the manuscript.

Funding: This research has received no external funding.

Data Availability Statement: No data applicable.

Acknowledgments: The authors express their gratitude to the dear referees, who wish to remain anonymous, and to the editors, for their helpful suggestions, all of which improved the final version of this paper.

Conflicts of Interest: The authors declare no conflict of interest.

References

1. Hilfer, R. *Applications of Fractional Calculus in Physics*; World Scientific Publishing Company: Singapore, 2000.
2. Gorenflo, R.; Mainardi, F. *Fractals and Fractional Calculus in Continuum Mechanics*; Carpinteri, A., Mainardi, F., Eds.; Springer: Wien, NY, USA, 1997; pp. 277–290.
3. Samko, S.; Kilbas, A.; Marichev, O. *Fractional Integrals and Derivatives: Theory and Applications*; Gordon and Breach: Amsterdam, The Netherlands, 1993.
4. Podlubny, I. *Fractional Differential Equations*; Academic Press: New York, NY, USA, 1999.
5. Oldham, K.B.; Spanier, J. *The Fractional Calculus*; Academic Press: New York, NY, USA, 1974.
6. Bagley, R.L.; Torvik, P.L. On the fractional calculus models of viscoelastic behaviour. *J. Rheol.* **1986**, *30*, 133–155. [\[CrossRef\]](#)
7. Atangana, A.; Baleanu, D. New fractional derivatives with nonlocal and non-singular kernel: Theory and application to heat transfer model. *Therm. Sci.* **2016**, *20*, 763–769. [\[CrossRef\]](#)
8. Al-Humedi, H.O.; Hasan, F.L. The Numerical Solutions of Nonlinear Time-Fractional Differential Equations by LMADM. *Iraqi J. Sci.* **2021**, 17–26. [\[CrossRef\]](#)
9. Abdoon, M.A. First Integral Method: A General Formula for Nonlinear Fractional Klein-Gordon Equation Using Advanced Computing Language. *Am. J. Comput. Math.* **2015**, *5*, 127–134. [\[CrossRef\]](#)
10. Hasan, F.L.; Abdoon, M.A. The generalized $(2 + 1)$ and $(3 + 1)$ -dimensional with advanced analytical wave solutions via computational applications. *Int. J. Nonlinear Anal. Appl.* **2021**, *12*, 1213–1241.
11. Abdoon, M.A.; Hasan, F.L.; Taha, N.E. Computational Technique to Study Analytical Solutions to the Fractional Modified KdV-Zakharov-Kuznetsov Equation. *Abstr. Appl. Anal.* **2022**, *2022*, 2162356. [\[CrossRef\]](#)
12. Elbadri, M. Initial Value Problems with Generalized Fractional Derivatives and Their Solutions via Generalized Laplace Decomposition Method. *Adv. Math. Phys.* **2022**, *2022*, 3586802. [\[CrossRef\]](#)
13. Chen, S.; Liu, Y.; Wei, L.; Guan, B. Exact solutions to fractional drinfel'd-sokolov-wilson equations. *Chin. J. Phys.* **2018**, *56*, 708–720. [\[CrossRef\]](#)
14. Kumar, D.; Seadawy, A.R.; Joardar, A.K. Modified Kudryashov method via new exact solutions for some conformable fractional differential equations arising in mathematical biology. *Chin. J. Phys.* **2018**, *56*, 75–85. [\[CrossRef\]](#)
15. Choi, J.H.; Kim, H. Soliton solutions for the space-time nonlinear partial differential equations with fractional-orders. *Chin. J. Phys.* **2017**, *55*, 556–565. [\[CrossRef\]](#)
16. Sarwar, S.; Iqbal, S. Stability analysis, dynamical behavior and analytical solutions of nonlinear fractional differential system arising in chemical reaction. *Chin. J. Phys.* **2018**, *56*, 374–384. [\[CrossRef\]](#)
17. Sadri, K.; Hosseini, K.; Hincal, E.; Baleanu, D.; Salahshour, S. A pseudo-operational collocation method for variable-order time-space fractional KdV-Burgers-Kuramoto equation. In *Mathematical Methods in the Applied Sciences*; John Wiley & Sons, Ltd.: Hoboken, NJ, USA, 2023.
18. Hosseini, K.; Samadani, F.; Kumar, D.; Faridi, M. New optical solitons of cubic-quartic nonlinear Schrödinger equation. *Optik* **2017**, *157*, 1101–1105. [\[CrossRef\]](#)
19. Hosseini, K.; Mayeli, P.; Ansari, R. Bright and singular soliton solutions of the conformable time-fractional Klein-Gordon equations with different nonlinearities. *Waves Random Complex Media* **2017**, *28*, 426–434. [\[CrossRef\]](#)
20. Hosseini, K.; Mayeli, P.; Bekir, A.; Guner, O. Density-Dependent Conformable Space-time Fractional Diffusion-Reaction Equation and Its Exact Solutions. *Commun. Theor. Phys.* **2018**, *69*, 1. [\[CrossRef\]](#)
21. Hosseini, K.; Kumar, D.; Kaplan, M.; Bejarbaneh, E.Y. New Exact Traveling Wave Solutions of the Unstable Nonlinear Schrödinger Equations. *Commun. Theor. Phys.* **2017**, *68*, 761. [\[CrossRef\]](#)
22. Hosseini, K.; Bekir, A.; Kaplan, M.; Güner, Ö. On a new technique for solving the nonlinear conformable time-fractional differential equations. *Opt. Quantum Electron.* **2017**, *49*, 343. [\[CrossRef\]](#)
23. Hosseini, K.; Manafian, J.; Samadani, F.; Foroutan, M.; Mirzazadeh, M.; Zhou, Q. Resonant optical solitons with perturbation terms and fractional temporal evolution using improved $\tan(\phi(\eta)/2)$ -expansion method and exp function approach. *Optik* **2018**, *158*, 933–939. [\[CrossRef\]](#)
24. Hosseini, K.; Xu, Y.J.; Mayeli, P.; Bekir, A.; Yao, P.; Zhou, Q.; Güner, O. A study on the conformable time-fractional Klein-Gordon equations with quadratic and cubic nonlinearities. *Optoelectron. Adv. Mater.* **2017**, *11*, 423–429.
25. Katugampola, U.N. New approach to a generalized fractional integral. *Appl. Math. Comput.* **2011**, *218*, 860–865. [\[CrossRef\]](#)
26. Katugampola, U.N. Existence and uniqueness results for a class of generalized fractional differential equations. *arXiv* **2014**, arXiv:1411.5229.
27. Almeida, R.; Malinowska, A.B.; Odziejewicz, T. Fractional Differential Equations with Dependence on the Caputo-Katugampola Derivative. *J. Comput. Nonlinear Dyn.* **2016**, *11*, 061017. [\[CrossRef\]](#)

28. Diethelm, K.; Ford, N.J.; Freed, A.D. A Predictor-Corrector Approach for the Numerical Solution of Fractional Differential Equations. *Nonlinear Dyn.* **2002**, *29*, 3–22. [\[CrossRef\]](#)
29. Odibat, Z.; Baleanu, D. Numerical simulation of initial value problems with generalized Caputo-type fractional derivatives. *Appl. Numer. Math.* **2020**, *156*, 94–105. [\[CrossRef\]](#)
30. Borah, M.; Singh, P.P.; Roy, B.K. Improved chaotic dynamics of a fractional order system, its chaos-suppressed synchronisation and circuit implementation. *Circ. Syst. Signal Process.* **2016**, *35*, 1871–1907. [\[CrossRef\]](#)
31. Vincent, U.; Kareem, S.; Nbandjo, B.N.; Njah, A. Quasi-synchronization dynamics of coupled and driven plasma oscillators. *Chaos, Solitons Fractals* **2015**, *70*, 85–94. [\[CrossRef\]](#)
32. Rashtchi, V.; Rahimpour, E.; Fotoohabadi, H. Parameter identification of transformer detailed model based on chaos optimisation algorithm. *IET Electr. Power Appl.* **2011**, *5*, 238–246. [\[CrossRef\]](#)
33. Lin, C.-J.; Yang, S.-K.; Yau, H.-T. Chaos suppression control of a coronary artery system with uncertainties by using variable structure control. *Comput. Math. Appl.* **2012**, *64*, 988–995. [\[CrossRef\]](#)
34. El-Gohary, A. Chaos and optimal control of cancer self-remission and tumor system steady states. *Chaos Solitons Fractals* **2008**, *37*, 1305–1316. [\[CrossRef\]](#)
35. Chen, D.; Zhao, W.; Sprott, J.C.; Ma, X. Application of Takagi–Sugeno fuzzy model to a class of chaotic synchronization and anti-synchronization. *Nonlinear Dyn.* **2013**, *73*, 1495–1505. [\[CrossRef\]](#)
36. Borah, M.; Roy, B.K. Dynamics of the fractional-order chaotic PMSG, its stabilisation using predictive control and circuit validation. *IET Electr. Power Appl.* **2017**, *11*, 707–716. [\[CrossRef\]](#)
37. Salah, E.; Saadeh, R.; Qazza, A.; Hatamleh, R. Direct Power Series Approach for Solving Nonlinear Initial Value Problems. *Axioms* **2023**, *12*, 111. [\[CrossRef\]](#)
38. Qazza, A.; Saadeh, R.; Salah, E. Solving fractional partial differential equations via a new scheme. *AIMS Math.* **2022**, *8*, 5318–5337. [\[CrossRef\]](#)
39. Salah, E.; Qazza, A.; Saadeh, R.; El-Ajou, A. A hybrid analytical technique for solving multi-dimensional time-fractional Navier-Stokes system. *AIMS Math.* **2023**, *8*, 1713–1736. [\[CrossRef\]](#)
40. Saadeh, R.; Qazza, A.; Amawi, K. A New Approach Using Integral Transform to Solve Cancer Models. *Fractal Fract.* **2022**, *6*, 490. [\[CrossRef\]](#)
41. Saadeh, R.; Ala'Yed, O.; Qazza, A. Analytical Solution of Coupled Hirota–Satsuma and KdV Equations. *Fractal Fract.* **2022**, *6*, 694. [\[CrossRef\]](#)

Disclaimer/Publisher's Note: The statements, opinions and data contained in all publications are solely those of the individual author(s) and contributor(s) and not of MDPI and/or the editor(s). MDPI and/or the editor(s) disclaim responsibility for any injury to people or property resulting from any ideas, methods, instructions or products referred to in the content.